# Anomalies in the Raman scattering spectra of piezoelectric $BaZnF_4$ crystals



1994 J. Phys.: Condens. Matter 6 10365

(http://iopscience.iop.org/0953-8984/6/47/019)

J. Phys.: Condens. Matter 6 (1994) 10365–10376. Printed in the UK

# Anomalies in the Raman scattering spectra of piezoelectric $BaZnF_4$ crystals

H N Bordallo†, A Bulou‡, R Almairac† and J Nouet‡

† Groupe de Dynamique des Phases Condensées, Université Montpellier II, URA CNRS 233, 34095 Montpellier, France

‡ Laboratoire de Physique de l'Etat Condensé, Université du Maine, URA CNRS 807, 72017 Le Mans, France

Received 28 July 1994

**Abstract.** A Raman scattering investigation of the piezoelectric compound $BaZnF_4$ has been performed in a wide temperature range. An accurate study of the characteristics, i.e. peak shifts, integrated intensities and half-widths, reveals anomalous changes in several spectral lines. The results are discussed on the basis of a breakdown of the $q = 0$ selection rules due to either a phase transition or structural disorder.

## 1. Introduction

$BaZnF_4$ is a member of the fluoride family $BaMF_4$, which includes $BaFeF_4$, $BaNiF_4$, $BaMnF_4$, $BaCoF_4$ and $BaMgF_4$, whose ferroelectric and antiferromagnetic properties are of significant interest. The crystal structure [1–6] of these compounds is built by planes of $MF_6$ octahedra perpendicular to the (010) cleavage direction, crystallizing in space group $A2_1am$–$C_{2v}^{12}$ ($Z = 4$). For all compounds, it has been shown [7] that the free dielectric constant along the $a$ axis obeys the Curie–Weiss law with an extrapolated paraelectric transition temperature above the melting point (prototype $Amam$—$D_{2h}^{17}$ phase). On the other hand, $BaMnF_4$ is the only one that undergoes an incommensurate structural phase transition at about 250 K.

The first report of Raman measurements on the biaxial piezoelectric $BaZnF_4$ was made by Quilichini and Poulet [8], who performed a complete zone-centre phonon analysis. According to their study all group-theoretically predicted modes have been assigned and the directional dispersion of each of the oblique optical phonons has been calculated and measured.

Later, Quilichini and co-workers [9] reported on the anomalous temperature dependences of the frequency and intensity of the mode at about 94 $cm^{-1}$, which 'softens' on heating, and its correlation with the virtual ferroelectric–paraelectric transition.

Our interest is in the low-temperature behaviour of a material that belongs to a family of compounds where a structural phase transition involving an incommensurate distortion occurs.

In this paper we present the results of a complete Raman-spectroscopy study, performed in a wide temperature range (~ 10–300 K) between 3 and 680 $cm^{-1}$ in $BaZnF_4$. This is a sensitive procedure to investigate structural phase transitions. An accurate analysis of the Raman spectra reveals an anomalous behaviour of some particular modes and evidence of disorder at 300 K.

0953-8984/94/4710365+12$19.50  

## 2. Experimental details

$BaZnF_4$ single crystals were prepared at the Laboratoire de Physique de l'Etat Condensé by the Bridgman–Stockbarger method. After orientation by x-ray techniques, the sample was cut and polished with faces oriented normal to the *abc* crystal axis, which is a reference setting where *a* is parallel to the binary axis.

Raman scattering spectra were carried out on a parallelepiped of dimensions 6, 6 and 4 mm, placed under secondary vacuum inside a refrigerator-cooled cryostat ROK 10–300. The sample temperature was controlled by a Variotemp HR1 and measured by a chromel–constantan thermocouple. For the excitation of the sample the 488 nm line of a Coherent Innova 90 Ar-ion laser was used, with a maximum power of 600 mW. A DILOR Z24 Raman spectrometer was used to analyse the light scattered in the classical 90° geometry, with a typical resolution of 2 $cm^{-1}$. At room temperature Raman spectra were recorded in the three planes $((a, b), (b, c), (c, a))$.

## 3. Results

### *3.1. Raman lines at room temperature*

From group theory the optical modes of $BaZnF_4$ at the Brillouin zone centre can be classified according to the $C_{2v}$ irreducible representations as follows:

$$11A_1 + 11B_2 + 6A_2 + 5B_1.$$

The Raman tensors for the $A_1$, $A_2$, $B_1$ and $B_2$ symmetries are [10]

$$A_1(a)\begin{bmatrix}\gamma & & \\ & \beta & \\ & & \alpha\end{bmatrix} \qquad A_2\begin{bmatrix}\cdot & & \\ & \cdot & \delta \\ & \delta & \cdot\end{bmatrix} \qquad B_1(c)\begin{bmatrix}\cdot & & \varepsilon \\ & \cdot & \\ \varepsilon & & \cdot\end{bmatrix} \qquad B_2(b)\begin{bmatrix}\cdot & \zeta & \\ \zeta & \cdot & \\ & & \cdot\end{bmatrix}$$

where the infrared-active modes are labelled (in parenthesis) by their polarization with respect to the crystallographic-axis directions.

It is known [11] that for both Raman and infrared active modes, the associated long-range macroscopic electric field can modify the polar phonon spectrum as a function of the direction of the phonon wave vector inside the crystal. Then, for the scattering geometries given in figure 1, the $b(aa)c(A_1)$, $b(ac)a(B_1)$ and $a(ba)c(B_2)$ spectra will correspond to transverse optical phonon (TO) modes only, whereas the $a(bb)c$, $b(cc)a$, $b(ab)a$ and $b(ab)c$ spectra will be associated with TO + LO (longitudinal optical) modes.

The frequencies of the modes in different symmetries, whose values result from a fitting procedure of the data with an appropriate number of Lorentzian components, are listed in table 1.

Because of the non-zero collection angle for the scattered beam, enumerating the observed modes is not an easy matter. A comparative analysis of the present spectra with earlier ones [8, 9], in the 50–450 $cm^{-1}$ frequency range, reveals that our observations agree with the former works within experimental error. Note that, at room temperature, the number of Raman lines does not exceed that predicted by the group-theory analysis. However, according to our data the mode at 115 $cm^{-1}$ in the $A_2$ symmetry attributed to a contamination in [8] seems to be real.

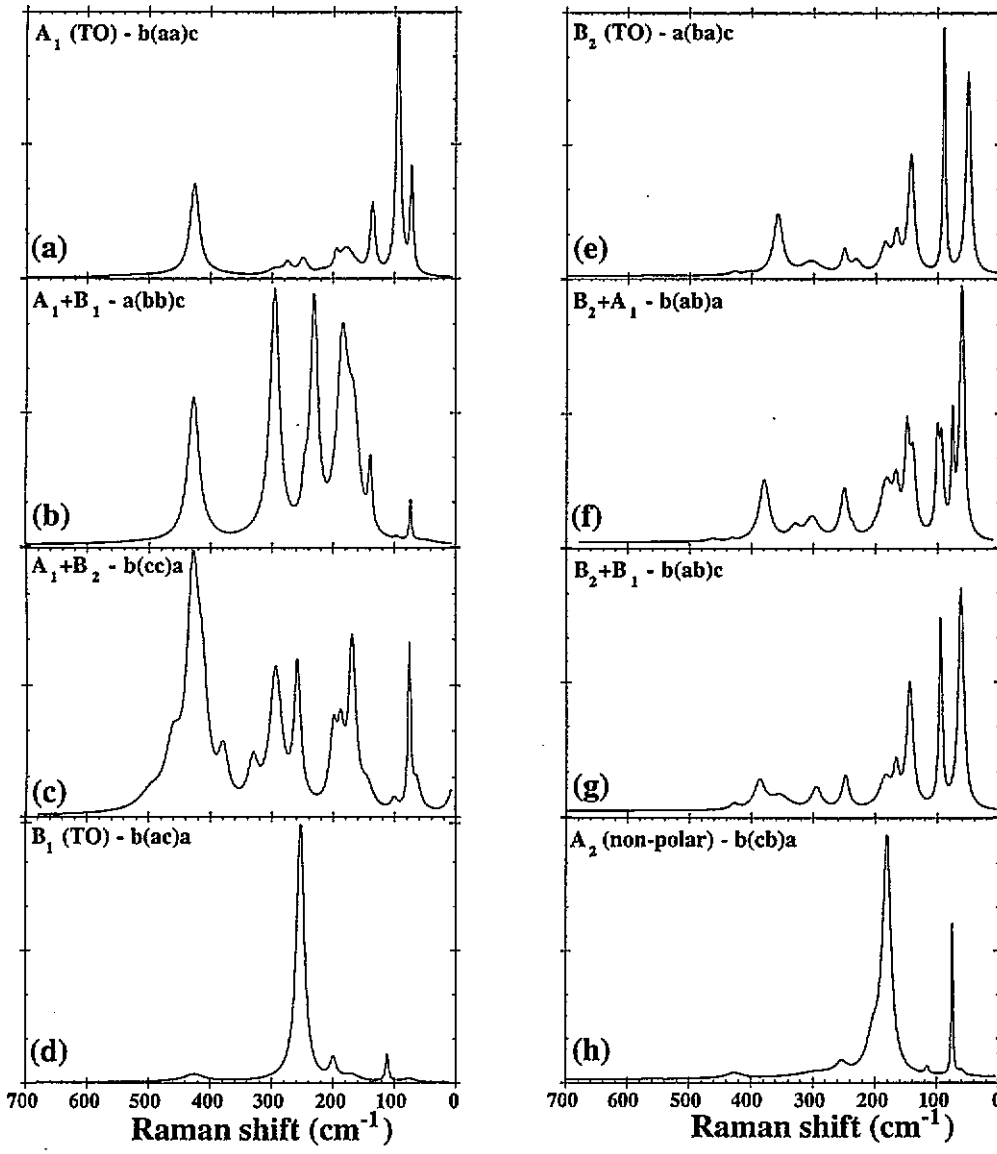


**Figure 1.** Raman spectra of $BaZnF_4$ at 300 K in the three planes ((*b*, *c*), (*a*, *c*), (*a*, *b*)): (a) TO modes of $A_1$—$h(aa)c$ symmetry; (b) $a(bb)c$ symmetry—TO + LO modes ($A_1 + B_1$); (c) $b(cc)a$ symmetry—TO + LO modes ($A_1 + B_2$); (d) TO mode of $B_1$—$b(ac)a$ symmetry; (e) TO mode of $B_2$—$a(ba)c$ symmetry; (f) $b(ab)a$ symmetry—TO+LO modes ($B_2 + A_1$); (g) $b(ab)c$ symmetry—TO+LO modes ($B_2 + B_1$); (h) the non-polar $A_2$ modes $b(cb)a$. All spectra were recorded with the same incident power.

A more interesting difference between our results and the previous ones is that two responses are observed in the frequency range below 50 $cm^{-1}$ in the $A_1$ symmetry (*cc*) (figure 2). The first is centred at 0 $cm^{-1}$, i.e. a quasielastic (QE) scattering, and the other is a broad one located at about 48 $cm^{-1}$. A detailed analysis of the temperature behaviour of these features is given in subsection 3.2.2.

**Table 1.** Frequencies of the TO modes $A_1$, $A_2$, $B_1$ and $B_2$, and of the TO+LO modes $A_1 + B_1$, $A_1 + B_2$, $B_2 + A_1$ and $B_2 + B_1$ of $BaZnF_4$ at room temperature. According to their Raman intensity the lines are labelled by: s = strong; m = medium or w = weak. The other abbreviations indicate the observation of a shoulder (sh) or a contamination (c) in the spectra.

| $A_1$ b(aa)c | $A_2$ b(cb)a | $B_1$ b(ac)a | $B_2$ a(ba)c | $A_1 + B_1$ a(bb)c | $A_1 + B_2$ b(cc)a | $B_2 + A_1$ b(ab)a | $B_2 + B_1$ b(ab)c |
|---|---|---|---|---|---|---|---|
| - | - | - | - | - | $0^{w}$ | - | - |
| - | - | - | - | - | $48^{w}$ | - | - |
| - | - | - | $52^{s}$ | $52^{c}$ | - | - | - |
| - | $62^{c}$ | - | - | - | $62^{m}$ | $61^{s}$ | $62^{s}$ |
| $72^{m}$ | $76^{m}$ | $75^{c}$ | - | $73^{m}$ | $75^{m}$ | $76^{s}$ | - |
| - | - | - | - | - | $86^{sh}$ | $94^{s}$ | - |
| $94^{s}$ | - | - | $91^{s}$ | $96^{w}$ | $100^{w}$ | $100^{s}$ | $95^{s}$ |
| - | $115^{w}$ | $111^{m}$ | - | - | $113^{c}$ | - | - |
| $136^{m}$ | - | - | - | $139^{m}$ | - | $139^{s}$ | - |
| - | - | | $144^{m}$ | - | $144^{sh}$ | $149^{s}$ | $145^{s}$ |
| $166^{w}$ | - | - | $168^{w}$ | $166^{s}$ | $169^{m}$ | $167^{s}$ | $167^{w}$ |
| $179^{w}$ | - | $170^{w}$ | - | $176^{s}$ | - | - | - |
| - | $181^{s}$ | - | $186^{w}$ | $185^{s}$ | $188^{m}$ | $183^{s}$ | $184^{w}$ |
| $195^{w}$ | - | - | - | - | - | - | - |
| - | $204^{w}$ | $200^{m}$ | - | - | $204^{m}$ | - | - |
| - | - | - | $232^{w}$ | $231^{s}$ | - | $237^{m}$ | - |
| $249^{w}$ | $253^{c}$ | $253^{s}$ | $251^{w}$ | $247^{s}$ | $248^{w}$ | $250^{s}$ | $248^{m}$ |
| - | - | - | - | - | $259^{m}$ | - | - |
| $275^{w}$ | - | - | - | $278^{sh}$ | - | - | - |
| $295^{w}$ | $292^{w}$ | - | - | $295^{s}$ | $294^{m}$ | - | $295^{m}$ |
| - | - | - | $304^{w}$ | - | - | $302^{m}$ | - |
| - | - | - | - | - | $331^{w}$ | $329^{m}$ | - |
| - | - | - | $359^{m}$ | - | - | - | $354^{w}$ |
| | - | - | - | - | $379^{w}$ | $379^{s}$ | $386^{m}$ |
| - | - | - | $405^{w}$ | - | $412^{s}$ | - | - |
| $426^{s}$ | $427^{w}$ | $425^{c}$ | $429^{c}$ | $427^{s}$ | $428^{s}$ | $431^{w}$ | $427^{w}$ |
| - | - | - | - | - | $461^{m}$ | $462^{w}$ | - |
| $510^{w}$ | - | - | - | $510^{w}$ | $497^{m}$ | - | - |

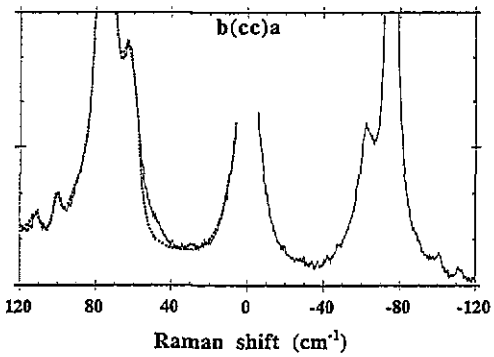


**Figure 2.** The detail of the low-frequency range of the Raman spectra $b(cc)a$ of $BaZnF_4$ at room temperature. The dotted line represents the result of a fitting procedure, on the Stokes side, without considering the mode at 48 cm$^{-1}$. Note also the clearly visible quasielastic (QE) scattering.

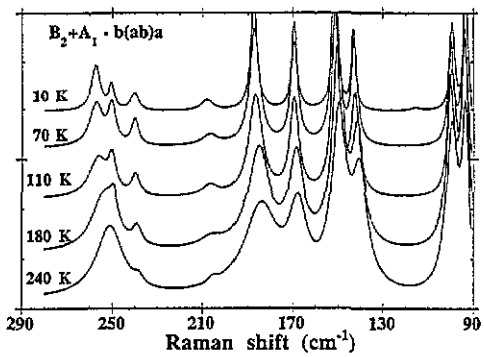


**Figure 3.** The temperature behaviour of the $b(ab)a$ Raman spectrum of $BaZnF_4$.

### *3.2. Raman spectra at low temperature*

The Raman spectra at low temperature (10–300 K) have been collected in the $(a, b)$ scattering plane for the four polarizations available, $b(cc)a$, $b(cb)a$, $b(ab)a$ and $b(ac)a$. It appears that they exhibit several unexpected features, such as

(i) a significant linewidth broadening against temperature of some lines;

(ii) the presence of extra (weak-intensity) lines at low temperature;

(iii) a dramatic decrease of the QE scattering (mentioned above) on approaching 100 K and

(iv) a softening of the line located at 48 cm$^{-1}$ (at room temperature).

These features are now presented in detail.

*3.2.1. An analysis of the spectra obtained in the whole frequency range.* Typical spectra are shown in figures 3–6.

When the temperature is lowered, a peculiar change is seen in the $b(ab)a$ scattering geometry (figure 3). The strong line whose peak frequency is at 250 cm$^{-1}$ at room temperature splits and transforms into two lines located at 251 and 258 cm$^{-1}$ at 10 K. This behaviour could have two different origins: either a slight polarization leak-through originating from the strong $B_1$ mode, normally observed in the $b(ac)a$ geometry, or a real splitting of the 250 cm$^{-1}$ line.

Excluding the first hypothesis, the asymmetric shape of the 250 cm$^{-1}$ line, for temperatures in the range 110–180 K, would suggest a possible coupling between two modes. In the same way, the temperature dependence of their frequency shifts seems to agree with this assumption, as can be noted in figure 7(*a*). The intensities and widths, deduced from the best-fit calculations of the spectra, are also represented in the same figure. It can be seen that the sum of the integrated intensities corrected for the Bose factor remains constant.

Except for the line at 48 cm$^{-1}$ (see subsection 3.2.2), no anomalous frequency shift against temperature is observed. As an illustrative example the characteristics of the $B_1$ mode at 253 cm$^{-1}$ are shown in figure 7(b).

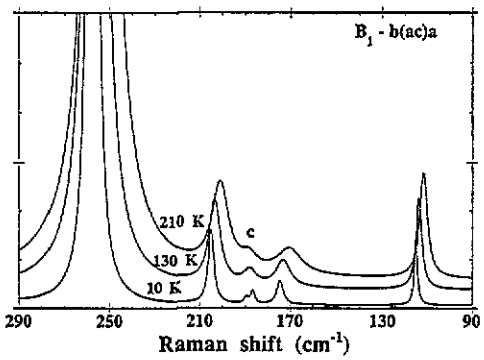


**Figure 4.** The temperature behaviour of the $b(ac)a$ Raman spectrum of $BaZnF_4$. A probable contamination is indicated by c.

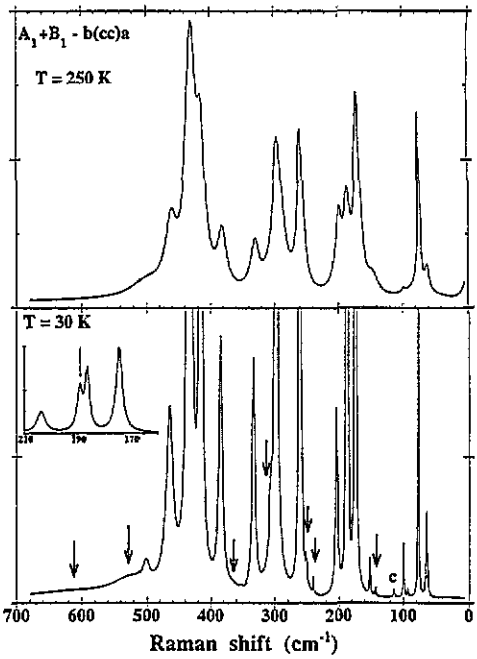


**Figure 5.** The temperature behaviour of the $b(cc)a$ Raman spectrum of $BaZnF_4$. The arrows indicate the new peaks and c indicates a probable contamination.

On the other hand, the evolution of the width versus temperature is not the same for the different lines studied. Some of them remain narrow in the whole temperature range, as does the mode at 75 $cm^{-1}$ in the $b(cc)a$ geometry or the TO mode $B_1$ at 111 $cm^{-1}$, which display a weak width variation. Others display a significant width narrowing at low temperature. An example is given in figure 7(b) for the intense $B_1$ mode at 253 $cm^{-1}$ (as a consequence, since the integrated intensity is almost temperature independent, its peak intensity becomes dramatically large at low temperature).

A similar behaviour was observed for the two sufficiently isolated lines at 294 and 428 $cm^{-1}$ in the $b(cc)a$ geometry, the widths of which change from 5 and 6 $cm^{-1}$ to 24 and 25 $cm^{-1}$, respectively.

In figures 5 and 6 it is observed that when the temperature decreases, many additional weak-intensity peaks arise below roughly 100 K: at 143, 189, 241, 251, 310, 365, 525 and 616 $cm^{-1}$ in $b(cc)a$ (figure 5), and at 152, 174, 240, 335, 384, 416 and 468 $cm^{-1}$ in $b(cb)a$ (figure 6).

Of course the possibility of spectral mixing due to contamination must be considered. However, the critical comparative analysis of the spectra leads to certainty that this effect alone cannot explain all the new lines appearing at low temperature, in particular the strong peak that arises at 189 $cm^{-1}$ in the $b(cc)a$ spectrum (see the inset of figure 5).

The appearance of only one strong band in the $b(ac)a$ spectra (figures 1 and 4) seems to be associated with the presence of only one mode, $B_{2g}$, expected for this representation in the virtual phase $D_{2h}$. Using the coordination of this irreducible representation, we obtain that this ionic motion consists of F(1) – F(2) displacement along the $c$ axis, i.e. a tilt of the octahedra around the $b$ axis (see figure 11).

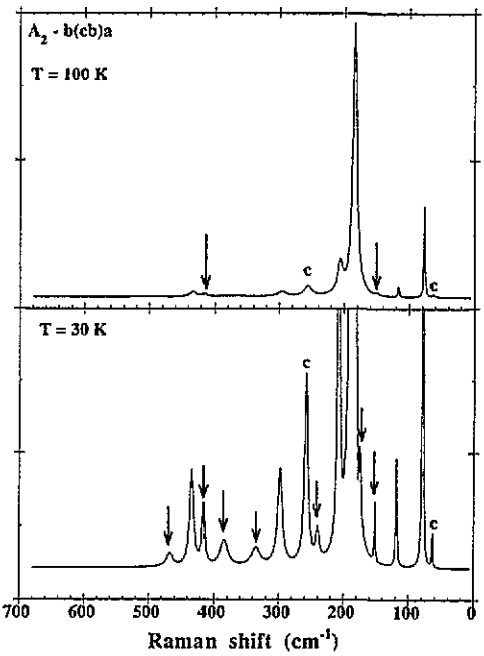


**Figure 6.** The temperature behaviour of the *b(cb)a* Raman spectrum of $BaZnF_4$. The arrows indicate the new peaks and c indicates a probable contamination.

*3.2.2. An analysis of the spectra obtained at low frequencies in the b(cc)a geometry.* In order to study the low-frequency signals observed in the *b(cc)a* geometry, several spectra from 3 to 120 $cm^{-1}$ were recorded in both the Stokes and anti-Stokes regions with long integration times. The Stokes parts of some spectra are shown in figure 8.

The first point to be considered is the presence of a low-frequency signal centred on zero, i.e. QE scattering or 'the central mode', which gradually disappears when the temperature is lowered. Another peculiar behaviour is associated with the mode at 48 $cm^{-1}$, which is observed only in the (*cc*) orientation (not in (*aa*) or (*bb*) orientations) and which strongly softens and shows a remarkable strength decrease on cooling.

The temperature dependence of the low-frequency peaks is shown in figure 9. An attempt to describe the 48 $cm^{-1}$ mode by the usual formula $\omega \sim (T - T_0)^{1/2}$ leads to $T_0 \sim -100$ K.

In order to obtain a better understanding of the origin of this weak peak the integrated intensities of the 48 $cm^{-1}$ and of the central modes were carefully analysed. This was possible since the spectra were measured rigorously under the same experimental conditions.

The intensities were obtained in two different ways: (i) for the mode located at 48 $cm^{-1}$, we used the results of the fitting procedure without correction of the Bose factor; (ii) for the central mode, first the Rayleigh component was subtracted from the measured spectra, then the signal was taken at one given frequency (8 $cm^{-1}$) and corrected for the background estimated by the level at 120 $cm^{-1}$. Finally the 75 $cm^{-1}$ mode was used as an internal monitor since it has been found not to be temperature dependent. This internal monitor was also used to measure the intensity of the 48 $cm^{-1}$ line. The precision is not very good but the results have proven to be useful as will be seen later.

The temperature dependences of the integrated intensities and widths of the QE scattering

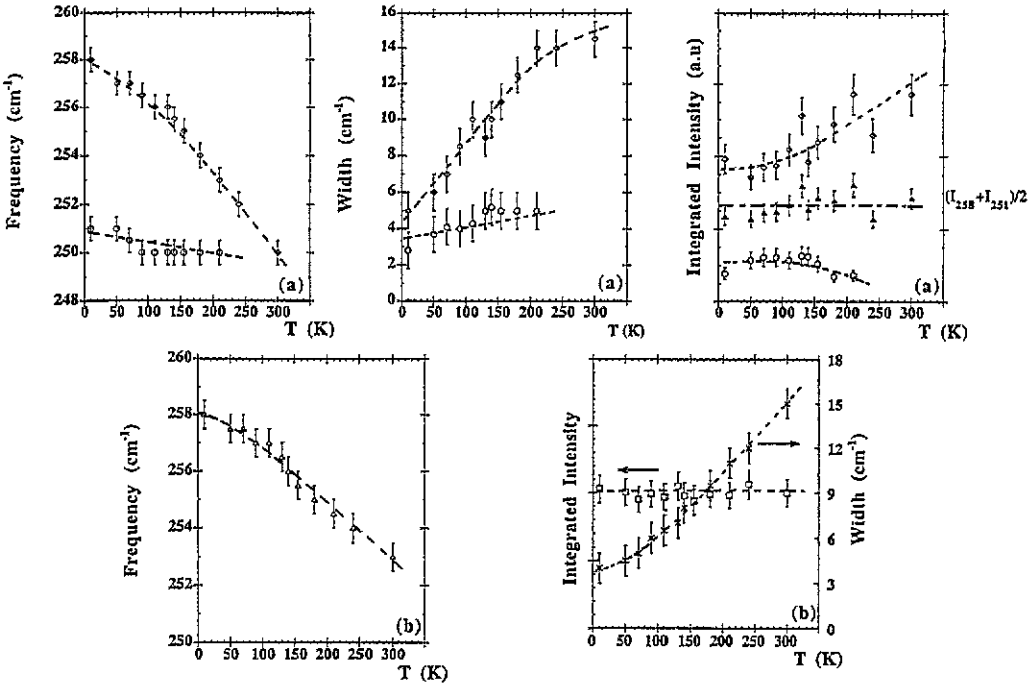


**Figure 7.** The temperature variation of parameters (frequency shift, width and integrated intensity corrected for the Bose factor) of the peculiar $B_2$—$b(ab)a$ modes located at 251 and 258 $cm^{-1}$ in (a) and of the intense $B_1$—$b(ac)a$ mode in (b). Dashed lines are guides for the eye.

and of the 48 $cm^{-1}$ mode are reported in figure 10.

Note that the disappearance of the central peak is not associated with narrowing of the width, which remains almost constant.

For the interpretation of the additional mode at about 48 $cm^{-1}$ we have examined the possibility that this unexpected line could be attributed to a second-order Raman-scattering process, in view of its notable decrease in intensity when temperature is lowered. This assumption must be excluded on the basis that the temperature variation of the Stokes intensity does not exhibit the so-called $(n+1)^2$ dependence (where $n$ represents the Bose–Einstein occupation factor for the phonons giving rise to such signals), as is clearly shown in figure 10(b).

Another particularity of this 'soft mode' concerns its linewidth. On cooling, it rapidly decreases. Below roughly 100 K the integrated intensity and the width remain constant. It seems therefore to be connected with the behaviour of the central component.

## 4. Discussion

One of the main results reported above is the presence of a QE signal that witnesses for the existence of some disorder in the structure, so we will first consider the ordering processes that can be expected in the $BaMF_4$ compounds. The basic idea is the particular organisation of $MF_6$ octahedra in these crystals.

Consider the highest-symmetry phase (paraelectric phase) from which $BaZnF_4$ is derived (figure 11(i)). The (virtual) transition from this phase to the ferroelectric $A2_1am$ phase

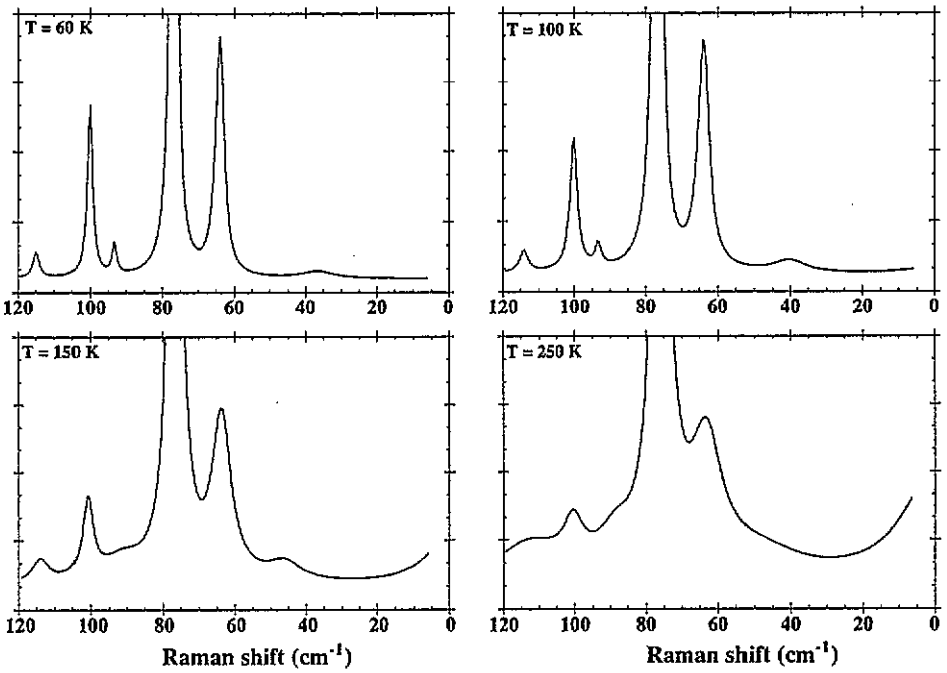


**Figure 8.** Representative $b(cc)a$ Stokes spectra of $BaZnF_4$, in the 0–120 cm$^{-1}$ region for the 60–250 K temperature range.

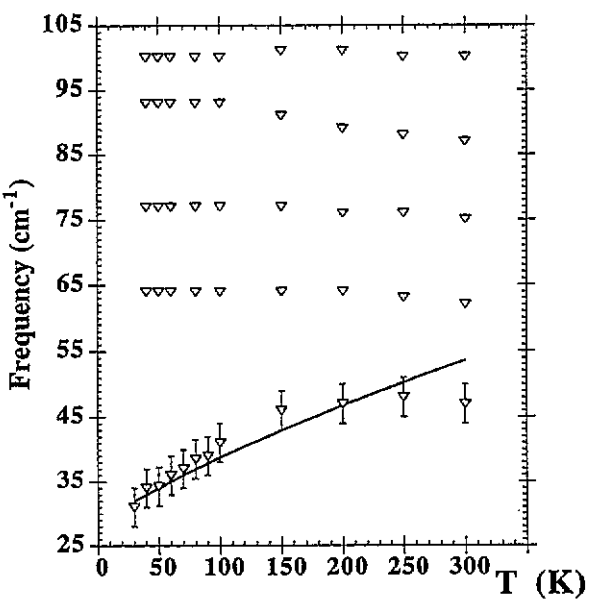


**Figure 9.** The temperature variation of peak positions of the low-frequency modes observed in the $b(cc)a$ spectra. The solid line represents a fit with the usual power law $\omega \sim (T - T_0)^{1/2}$ with $T_0 \sim -100$ K.

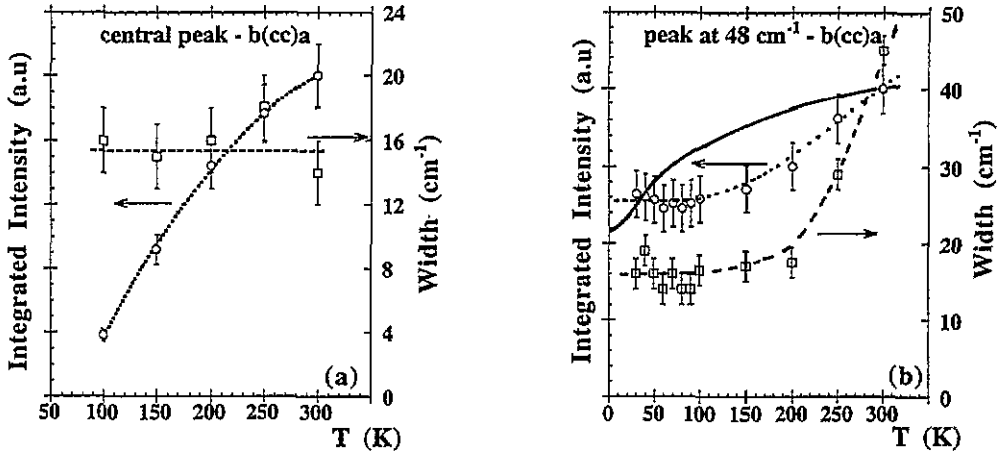


**Figure 10.** The temperature dependence of the integrated Raman intensities (monitored by the intensity of the 75 $cm^{-1}$ line) and widths, for the central mode (a) and for the mode located at 48 $cm^{-1}$ (b). In (b) the full line shows the integrated Raman intensity as a function of temperature for a second-order scattering process. Dashed lines are guides for the eye.

would be induced by the softening of a $B_{1u}$, mode which corresponds to rotations of $MF_6$ octahedra around the *c* axis with a gearing mechanism along the *a* axis as indicated by arrows in figure 11(i). This movement results in a more compact arrangement of the ions with a net shortening of the *a* parameter along the chain axis, as is shown by figure 11(ii), but short-range interactions between $F^-$ and $Ba^{2+}$ ions prevent a too large rotation of the octahedra.

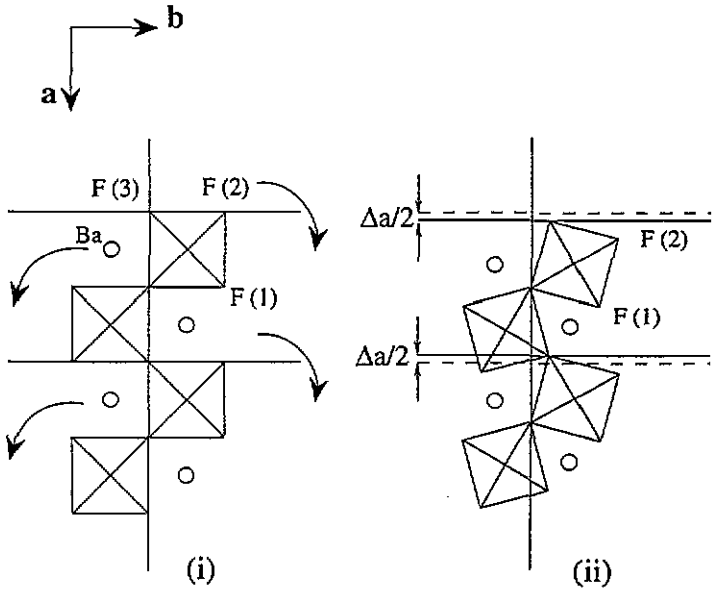


**Figure 11.** Representations of the $BaZnF_4$ structure (with schematization of the $ZnF_6$ octahedra): (i) the ideal high-symmetry phase with $D_{2h}$ point group and (ii) the room-temperature phase with $C_{2v}$ point group.

During further cooling, the crystal can no longer gain in compactness and energy by this process. The only and easy way to gain and reduce again the cell volume is a tilting of the octahedra around axes perpendicular to the $c$ direction. This leads to a doubling of the $c$ parameter. However no clear and simple correlation of these movements appears in the $(a, b)$ plane.

From the above considerations diffuse scattering would be expected in the $(\xi\ \zeta\ 0.5)$ reciprocal space planes. As the sheets of octahedra are weakly bound in the $b$ direction, one expects to observe streaks elongated along $b^*$. This hypothesis is consistent with the results obtained by Edwardson *et al* [12] on the basis of a model of dynamics in $BaMnF_4$. These authors have found instabilities around (0.32 0.5 0.5) and (0.35 0 0.5), all points located on the $(\sim 0.34\ \zeta\ 0.5)$ line. Our x-ray results [13] obtained on $BaZnF_4$ by photographs, using an oscillating-crystal method at room temperature, display weak and broad diffuse streaks parallel to $b^*$ corresponding to $(0.5\ \zeta\ 0.5)$, in agreement with the above discussion. As no transition has ever been reported at low temperature in $BaZnF_4$, it would correspond to some disorder. This result is in full agreement with the QE signal observed in the Raman $a(cc)b$ spectrum, i.e. at room temperature the crystal presents a disorder presumably related to tilts or jumps of the $MF_6$ octahedra, which results in a doubling of the $c$ parameter.

Together with the QE scattering, the linewidth variations observed for some modes in our Raman results can also be correlated to the occurrence of disorder. In the ordered crystal the lines are well defined (narrow) whereas in the disordered state the response corresponds to the sum of all the possible states, thus resulting in larger linewidths.

Now we turn to the interpretation of the weak additional Raman lines below 100 K. These lines must be assigned to a breakdown of the $q = 0$ selection rules. Different hypotheses can be considered. First they can suggest that a monoclinic shear is produced. It will be marked by an increase of the number of Raman lines because, due to the decrease of the number of irreducible representations, a release of the polarization rules takes place. Another possibility would be the breaking of the $C_{2v}$ $(a, b, c)$ selection rules because the modes of the Brillouin zone boundary become active. This represents a cell doubling along the $c$ direction. This second possibility is in agreement with the x-ray observations of diffuse scattering at room temperature.

The present Raman study leads us to argue the possibility of a structural phase transition. Such a transition can be expected to be typical of the $BaMF_4$-type structure, so it could be similar to the commensurate–incommensurate transition of $BaMnF_4$, where the point-group symmetry of the incommensurate phase is monoclinic with a very small departure of the $\beta$ angle from 90° [14] (the existence of twin monoclinic domains can result in an apparent incorrect symmetry at first sight, if the proportion is not far from 50/50).

An alternative interpretation might arise if the space group and cell parameters were preserved and if we supposed that no transition occurred in this compound. However this supposition gives an apparent contradiction between the structural determination and the Raman results. In order to solve this disagreement we remark that the Raman time scale is short with respect to the time scale applying for a structure determination, so that the symmetry found by the second method is an average of the symmetry corresponding to the first one. Assuming that the disorder corresponds to tilts of the $MF_6$ octahedra around an axis of the (001) plane, the Raman spectra would give the response of tilted system whereas the x-ray structural description would correspond to the average over all tilted positions.

Finally the behaviour of the 48 $cm^{-1}$ mode is also connected to the occurrence of disorder at high temperature, as has been shown in subsection 3.2.2. However the soft character of this weak mode, which could give a displacive phase transition under some favourable conditions—perhaps pressure—is somewhat unexpected and puzzling.

## 5. Conclusion

From these results it appears that $BaZnF_4$, which belongs to a family of compounds where an incommensurate phase transition has been observed ($BaMnF_4$) and which was considered as a reference, exhibits an anomalous behaviour at low temperature.

We have proposed an interpretation of the width and intensity behaviours, based on the presence of thermally activated disorder. Concerning the breakdown of the $q = 0$ selection rules at low temperatures, two alternative interpretations have been suggested. In the first case we suppose that a phase transition takes place in the crystal. In the second one, where no phase transition is involved, we are left with an apparent contradiction for which an explanation has been proposed.

Further experimental investigations by inelastic neutron scattering are now in progress in order to decide between these two alternatives.

## Acknowledgments

It is a pleasure for us to thank J L Sauvajol and G De Nunzio for helpful discussions and G Niesseron for the crystal growth. We also wish to acknowledge J Lapasset for the structure refinement by x-ray diffraction ($r = 3\%$) of $BaZnF_4$. One of us (HNB) is grateful to the Brazilian Conselho Nacional de Desenvolvimento Científico e Tecnológico—CNPq for its financial support.

## References

[1] Lapasset J 1994 private communication
[2] von Schnering H G and Bleckmann P 1968 *Naturwiss.* **55** 343
[3] de Pape R and Ravez J 1966 *Bull. Soc. Chim. France* **10** 3283
[4] Cousseins J C and Samouël M 1967 *C. R. Acad. Sci. Paris* C **265** 1121
[5] Keve E T, Abrahams S C and Bernstein J L 1969 *J. Chem. Phys.* **51** 4928
[6] Keve E T, Abrahams S C and Bernstein J L 1970 *J. Chem. Phys.* **53** 3279
[7] Di Domenico M Jr, Eibschütz M, Guggenheim H J and Camlibel I 1969 *Solid State Commun.* **7** 1119
[8] Quilichini M and Poulet H 1974 *Phys. Status Solidi* b **62** 501
[9] Quilichini M, Ryan J F, Scott J F and Guggenheim H J 1975 *Solid State Commun.* **16** 471
[10] Lockwood D J, Murray A F and Rowell N L 1981 *J. Phys. C: Solid State Phys.* **14** 753
[11] Poulet H 1955 *Ann. Phys. (Paris)* **10** 908
[12] Edwardson P J, Katkanant V and Hardy J R 1987 *Solid State Commun.* **64** 625
[13] Almairac R to be published
[14] Ryan T W 1986 *J. Phys. C: Solid State Phys.* **19** 1097